Journal of Nanoparticle Research **1:** 353–368, 1999.

Formation of silver and gold dendrimer nanocomposites

Lajos Balogh[1], Regina Valluzzi[2], Kenneth S. Laverdure[3], Samuel P. Gido[3], Gary L. Hagnauer[4] and Donald A. Tomalia[1,5]
[1]*Center for Biologic Nanotechnology, University of Michigan, Ann Arbor, MI 48109-0533, USA (Tel.: 734 615 0623; Fax: 734 615 0621);* [2]*Tufts Biotechnology Center, Department of Chemical Technology, Medford, MA 02155, USA;* [3]*University of Massachusetts, Amherst, Polymer Science and Engineering, Amherst, MA 01003,USA;* [4]*AMSRL-WM-MA, US Army Research Laboratory, APG, MD 21005, USA;* [5]*ARL-MMI Dendritic Polymers Center of Excellence Michigan Molecular Institute, Midland, MI 48640-2696, USA*

Received 7 July 1998; accepted in revised form 10 March 1999

Key words: dendrimers, nanoparticles, polymer-inorganic nanocomposites, templates

Abstract

Structural types of dendrimer nanocomposites have been studied and the respective formation mechanisms have been described, with illustration of nanocomposites formed from poly(amidoamine) PAMAM dendrimers and zerovalent metals, such as gold and silver. Structure of $\{(Au(0))_n$-PAMAM$\}$ and $\{(Ag(0))_n$-PAMAM$\}$ gold and silver dendrimer nanocomposites was found to be the function of the dendrimer structure and surface groups as well as the formation mechanism and the chemistry involved. Three different types of single nanocomposite architectures have been identified, such as internal ('I'), external ('E') and mixed ('M') type nanocomposites. Both the organic and inorganic phase could form nanosized pseudo-continuous phases while the other components are dispersed at the molecular or atomic level either in the interior or on the surface of the template/container. Single units of these nanocomposites may be used as building blocks in the synthesis of nanostructured materials.

Introduction

Nanotechnology will be a significant driving force in the 21st century technological revolution. This emerging interdisciplinary area requires a new way of thinking as well as the input of both experimental and theoretical scientists from the areas of physics, chemistry and materials science [1,2].

Cluster science is devoted to understanding the changes in fundamental properties of materials as a function of size, evolving from isolated atoms or small molecules to a bulk phase [3]. The term 'cluster' and 'micro-cluster' are usually used to describe aggregations of atoms that are too large to be referred to as molecules and too small to resemble small pieces of crystals. Well defined metal clusters [4,5] are considered as new perspectives in future nanoelectronics [6]. These aggregates generally do not have the same structure or atomic arrangement as a bulk solid, and can change structure with the addition of just one or a few atoms. As the number of atoms (and their degree of freedom) increases, eventually a crystal-like structure may be established [7].

Fabrication of microscale devices requires nanolevel control over their structural materials. Numerous approaches are currently used to control the size and polydispersity of nanosized particles such as preparative approaches, in which one attempts to optimize

reaction conditions for required structures [8], the colloid chemical approach [9] utilizing regular or inverse micelles [10], or Langmuir–Blodgett films [11]. Nanostructured materials have been made by biomimetic methods [12], in synthetic [13] and natural membranes [14], proteins [15] and DNA [16]. Stabilization with protective polymers [17,18], utilizing phase-separation in ionomers [19,20], or block copolymers [21,22], functionalizing inorganic cluster surfaces with dendrons [23]. In addition, filling carbon nanotubes with Ag, Au and gold chloride [24] were also reported. Highly ordered polymer-inorganic nanocomposites were also synthesized via monomer self-assembly [25].

Presently, particle size polydispersity prevents construction of well-defined two- or three-dimensional structures [26]. A breakthrough in this area would be of enormous scientific and practical significance in the fields of information technology, communication hardware, electronics, optics as well as many other fields.

Since the first report [27] by Tomalia et al. in 1985 it has been known, that dendrimers are able to form complexes with a great variety of ions and compounds [27–30]. The concept of dendrimer nanocomposites [31,32] is based on the immobilization of preorganized metal ions. For the first time, this concept has been demonstrated on the example of metal sulfide dendrimer hybrid nanocomposites [32] and it has quickly produced further examples [33–36].

According to the original dendrimer nanocomposite (DNC) concept, a dendrimer is used first as a *template* to preorganize ions or small molecules. Then, the dendrimers are used as a *reactor*, and the preorganized precursors are immobilized by an *in-situ* reaction which stabilize domains of atoms or molecular components (either inorganic compounds or elemental metals) and the used macromolecules with respect to each other. In that phase, the dendrimer host becomes a container (Scheme I).

Control of size, shape and size-distribution is achieved by employing well-defined dendrimers as templates, because dendrimers have a homogenous ligand-field as opposed to micelles or inverted micelles.

Preorganization may occur by any guest–host mechanism, such as complex formation by ligand/metal-ion interactions, salt formation, acid–base, donor–acceptor interactions, etc. Due to the large number of available binding sites within the dendrimers and the many possible overlapping equilibrium processes (involving several different geometries), binding of the guest to the host usually appears as a non-stoichiometric process. This preorganization results in a dendrimer–precursor conjugate, which is in dynamic equilibrium with the template and the precursor reactants. The dynamic

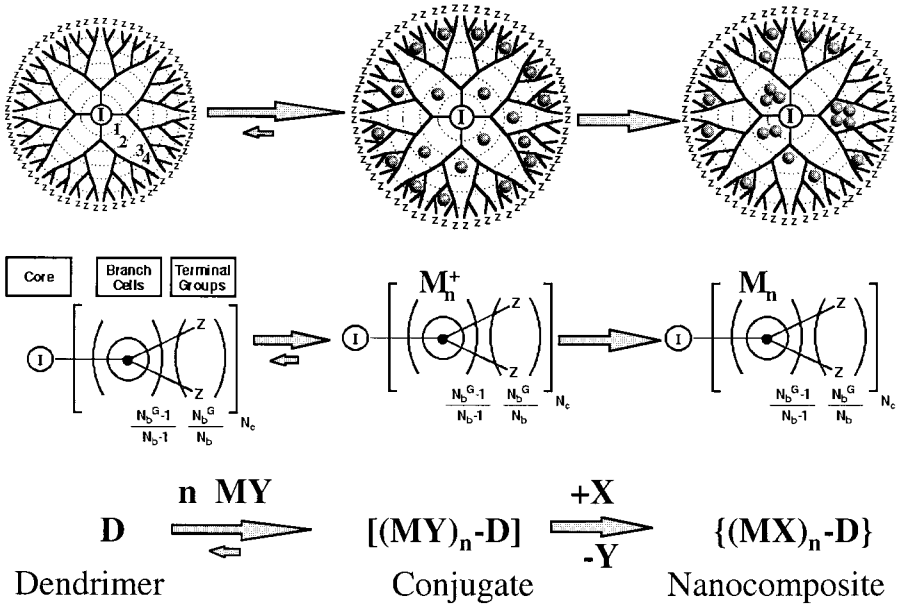

Scheme I. Preparation of DNCs by reactive encapsulation.

equilibrium ensures equal distribution of the precursor molecules between all the equivalent ligands and diffusion provides a homogenous distribution of ions among the dendrimer reactors.

The second step in the dendrimer nanocomposite formation is a reaction (or reaction sequence) that yields the desired product from the preorganized atoms/molecules. This reaction product must be insoluble in the media used as solvent for the templating dendrimer, just like in the reduction of the complexed Cu(II) ions into Cu(0) in an aqueous solution of the PAMAM dendrimer [33,34] or transformation of the complexed Cu(II) ions or Cd(II) ions in the solution of an appropriate PAMAM into CuS [32] or CdS [35]. After this step, the dendrimer acts as a container, and becomes the organic component of a hybrid material. This physical or physicochemical complex entrapment [37] of the inorganic component may occur either as a result of interactions of the *in-situ* generated compound(s) with the binding functions of the PAMAM dendrimer, or an increase in the size of the reaction product compared to the preorganized form, and/or formation of new intermolecular interactions between the product molecules/atoms of the guest.

It is important to emphasize the difference between conventional nanoparticles and dendrimer based nanocomposites. Conventional ('hard') metal clusters are *microcrystalline* and usually are composed of hundreds of metal atoms that are bonded to each other with metallic bonds. To hinder further crystal growth and secondary clustering, surface of these nanoparticles are usually deactivated by stabilizers [38]. Dendrimer nanocomposites are ('soft') hybrid materials that are composed of inorganic domains of small number of atoms/molecules dispersed within or on the dendrimers while the covalent branches and connectors of dendrimers act as separators. Due to this unique fine structure, DNCs are often amorphous. They usually have a very weak internal crystalline order whereas the size of the inorganic domains is comparable to the size of the unit cell [33,40].

Three major guest–host arrangements can be classified according to the location of the dispersed inorganic phase compared to the dendrimer. Each single nanocomposite particle consists of *one* dendritic molecule and the dispersed inorganic guest atom or molecule. Thus, dendrimer nanocomposites may form internal ('I'), external ('E') or mixed ('M') type single nanocomposite structures (Scheme II).

Regular/classic composites consist of at least one macroscopically continuous phase as well as one or more components dispersed on a microscopic scale. In DNCs, the size of the host is of nanoscopic scale. Due to the atomic/molecular level dispersion of the inorganic and organic matter, dendrimer based nanocomposites display unique physical and chemical properties. These materials are real composites with no covalent interaction between their components. Dendrimer nanocomposites (DNCs), in accordance with their composite character, display physical and chemical properties that are characteristic of both the nanosized host and the nanodispersed guest. For example, while solubility is mainly determined by the container dendrimer molecules, {Cu(0)-PAMAM} nanocomposites display the optical properties of the nanodispersed very small copper metal domains [33,34]. As a

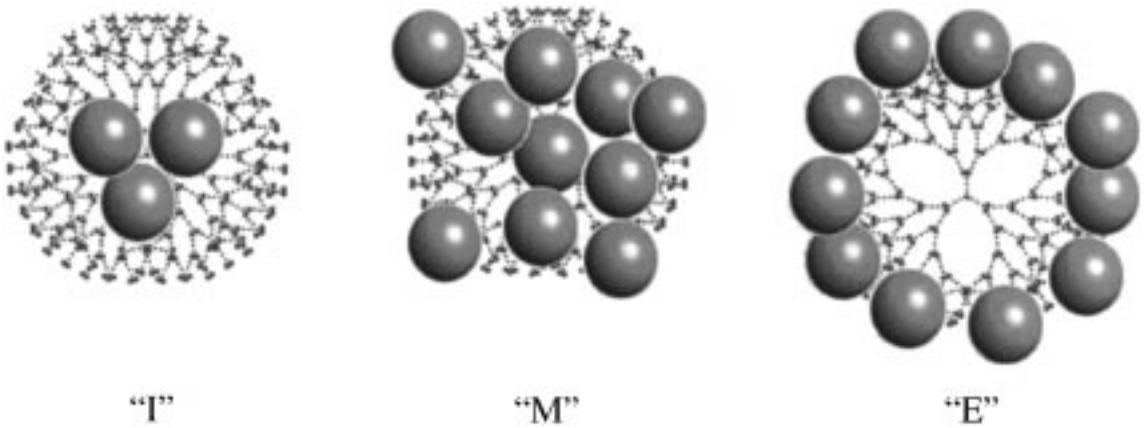

Scheme II. Single and one component internal ('I'), mixed ('M') and external ('E') type DNCs structures. The spheres represent individual atoms or molecules.

result of the intimate atomic/molecular level interaction between the components, new properties are also created, e.g., aqueous solutions of $\{Cu(0)_{10}$-PAMAM-E4$\}$ nanocomposites had no plasmon peaks in their visible spectrum [33].

In DNCs, most of the interactions between guest atoms and their microenvironment (metal–metal and metal–solvent interactions) are substituted with the metal–dendrimer and dendrimer–solvent interactions. For this reason, DNC solutions may be stable for very long time in appropriately selected solvent systems. This feature is especially important in the nanoscopic region, where decreasing size results in increasing number of surface atoms, therefore in an increasing role of surface interactions. However, what can be considered as the 'surface' of a DNC, is still to be defined.

Experimental

Materials

In this work, ethylenediamine core poly(amidoamine) (PAMAM) dendrimers were used. Amino surface generation 5 PAMAM dendrimer (128 terminal primary amino groups and 126 internal tertiary amino groups) based on ethylenediamine core (Mn = 28,826) and carboxylate surface generation 5 PAMAM dendrimer (256 terminal −COOH and 126 internal tertiary amino groups, Mn = 50,865) was purchased from Dendritech and was used without further purification. Technical grade chemicals were used (>85% generational dendritic purity). TRIS-modified dendrimers were synthesized by standard literature procedures. Generation four TRIS-modified dendrimer (Mn = 18,636) was provided by Dr. D.R. Swanson, MMI (Table 1).

These combinations offered cationic and strong electrondonor $-NH_2$, polar and weak protondonor $-C(CH_2OH)_3$ groups as well as anionic carboxylate terminal groups with a comparable number of nitrogen ligands.

High purity CH_3COOAg, $AgNO_3$, $HAuCl_4$, $NaAuCl_4$ and hydrazine (30% in H_2O) were purchased from Aldrich and were used without further purification.

Techniques

The starting materials and the obtained products were carefully characterized by different analytical techniques. UV–visible spectra were obtained on a Cary 1E spectrophotometer at room temperature between 200 and 900 nm in a Suprasil 300 quartz cell ($L = 1$ mm). ^1H and ^{13}C NMR measurements of the dendrimers were carried out by a Varian Unity 300 multinuclear spectrometer equipped with a temperature controller. Size Exclusion Chromatography was performed on three TSK gel columns (4000, 3000 and 2000) using a Waters 510 pump with a Wyatt Technology Dawn DSP-F MALLS and Wyatt Technology 903 interferometric refractometer and a Waters 510 pump with a Waters 410 differential refractometer respectively.

A Phillips EM301 instrument was applied for transmission electron-microscopy (TEM) of nanocomposites using Formvar coated carbon grids after appropriate dilution. High resolution TEM was preformed using a JEOL JEM-2000-FX and JEM-3010 transmission electron microscopes. A glove box with a dry nitrogen atmosphere was used to prevent change of oxidation state of the metals within the dendrimer nanocomposites during sample preparation. The grids used for HRTEM were carbon supported film 400-mesh copper grids. The carbon films were rendered hydrophilic by plasma etchings. In several cases polystyrene spheres (diameter = 91 ± 6 nm) were used for calibration. Grids were scanned on the 2000-FX operated at 200 kV accelerating voltage then the most suitable grid was transferred to the JEM-3010 and imaged at 300 kV accelerating voltage. The original high-resolution micrographs were taken at 100,000–150,000 magnifications and subsequently enlarged

Table 1. Comparison of PAMAM dendrimers used

Shorthand	Surface	No. of subsurface tertiary nitrogens	Possible position of ion bonding
E4.TRIS	64 $-C(CH_2OH)_3$	62	interior
E5.NH_2	128 $-NH_2$	126	interior + exterior
E5.COOH	256 −COOH	126	interior + exterior

three times on the enlarger and zoomed further on the scanner.

Silver content was determined by atomic absorption measurements at the Independent Testing Laboratory of the Saginaw Valley University, MI.

Preparation of silver–dendrimer nanocomposites

For silver complexation experiments typically silver acetate was selected because of its low solubility in water. Thus, a typical procedure for example #1 was as follows: to 0.209 g (1.25×10^{-3} mol) silver acetate powder and 0.746 g (4.0×10^{-5} mol) PAMAM E4.TRIS 20 ml of water was measured in a vial and shaken until the solid dissolved (metal/dendrimer = 31.29).

Photolysis of the colorless solution over an extended time, yielded a dark brown silver nanocomposite solution, which proved to be stable even in more concentrated (10% w/w nanocomposite) nanocomposite solutions.

For example #2, to 15 ml of water 5.007 g aqueous solution of 0.524 g (1.034×10^{-5} mol) PAMAM_E5.COONa (Mn = 50,865) was added and shaken with excess of (0.427 g) Ag-acetate overnight. This procedure resulted in dissolving 0.251 g (1.50×10^{-3} mol) inorganic salt. The undissolved material was removed by filtration. To the resulting dark tan solution, that contained the silver-salt of the anionic PAMAM and sodium acetate, calculated amount (150 ml) of 30% aqueous hydrazine solution was added by means of a microsyringe during vigorous stirring. The dark brown solution was stored at room temperature.

Preparation of gold–dendrimer nanocomposites

Preparation of gold–dendrimer complexes were carried out in aqueous solution by mixing dilute (1 mM) aqueous solutions of $[AuCl_4]^-$ with the aqueous solution of the PAMAM dendrimer at a molar ratio of ten gold atoms per dendrimer. The yellow $[AuCl_4]^-$ solution lost its color immediately upon mixing with the PAMAM indicating the formation of a salt between the dendrimer tertiary nitrogen and the complex gold anion. Stable dendrimer gold nanocomposites were prepared by reducing the PAMAM – tetrachloroaurate polysalts at room temperature with a slight excess of hydrazine (50 mol% excess). Upon addition of the hydrazine solution to the dendrimer–gold conjugate, a color change from slightly yellow to deep red indicated the reduction of gold anions coordinated to the dendrimer nitrogens into zerovalent gold. The solutions were transparent and displayed no Tyndall effect. Control solutions without dendrimers resulted in an immediate gray precipitate.

Concentrations of the final nanocomposite solutions were 3.78 g/L for dendrimer and 0.5 and 0.58 g/L for gold.

We have stored our dendrimer–gold and dendrimer–silver nanocomposites for more than 120 days at room temperature. They were stable and did not coagulate.

Results and discussion

Dendrimers are perfect organic templates because of their well-defined, predetermined and variable composition, symmetric structure, monodisperse distribution, size, controlled shape, and chemically variable interior and exterior. Dendrimers with different composition and architecture can interact and contain a wide variety of *in-situ* synthesized compounds, while the surface of the dendrimers may still be available for further modifications. Thus, using dendrimers as templates, reactors and containers, ideally the size, shape and size-distribution of the dispersed material(s) are created, determined and controlled by an appropriate dendritic polymer. Countless combinations are possible between metal cations or anions and dendrimers, therefore we limit our examples to aqueous solutions of nearly spherical ethylenediamine core poly(amidoamine) (PAMAM) dendrimers (see Table 1) with container properties [37] in conjunction with silver(I) cations and gold(III) ions in the form of complex $[AuCl_4]^-$ (tetrachloroaurate) anions and below the saturation level of the templates. Our conclusions, however, will be useful and demonstrative for many other similar systems.

In PAMAM dendrimers (Scheme I) the branching points are N^3 tertiary nitrogens possessing all the ability to enter either acid/base reactions or act as electron donor ligands in the complexation of metal ions. Thus, in aqueous solutions of the pure PAMAM the interior is protonated and has a cationic character, except for extreme conditions. The exterior of the molecule, however, may either be hydrophobic (e.g., $-n$-alkyl) or hydrophilic, the latter may possess cationic ($-NH_2$), neutral ($-CH_2OH$) or anionic ($-COOH$) terminal groups.

There are four major factors to consider as key to the successful imaging of size, shape and size-distribution

when using templates:

(i) composition, architecture and quality of the template used;
(ii) the effectiveness/effectivity of filling the template with the appropriate precursor (nature of preorganizing interactions, equilibrium constants, total capacity, degree of loading, etc.);
(iii) the nature (order, mechanism and kinetics) of the immobilizing reaction producing *in-situ*-generated nanodispersed domains of the guest molecules, i.e., the formation of the final composition;
(iv) the 'afterlife' of the nanoparticles (inherent stability, type, resulting interparticle interactions, association, self-assembly, etc.) that may result in secondary products and architectures according to the physics and chemistry of the nanocomposites formed, i.e., the finalization of the structure of the DNC.

Every above mentioned step has its specific character and its own time-scale that may be different in the case of different nanocomposites. We are going to focus on primarily on the first three factors, since (iv) requires much more research in order to collect sufficient amount of reliable information that will afford at least a certain degree of generalization.

Considering, that either cations or anions may serve as precursors, the following three major preorganization mechanisms are considered in this paper:

Examples of formation mechanisms

DNC-1: *Conjugation by complexation followed by a zero-order monomolecular reaction*
Example. Complexation of silver cations in neutral (TRIS) surface dendrimers followed by photolysis into an interior ('I') type $\{Ag(0)\}_I$ nanocomposite;

DNC-2: *Conjugation by dendrimer carboxylate salt formation followed by a bimolecular reaction*
Example. Binding of silver cations on carboxylate terminated PAMAMs followed by reduction into a dominantly exterior ('E') type $\{Ag(0)\}_E$ nanocomposite;

DNC-3: *Salt formation between complex anions and cationic sites of PAMAM dendrimers followed by a bimolecular reaction*
Example. Salt formation between tetrachloroaurate anions and PAMAM dendrimers followed by reduction into dendrimer gold nanocomposites. This reaction route may provide both interior and exterior types, but usually results in mixed ('M') type $\{Au(0)\}_M$ nanocomposites.

DNC-1 example: *Complexation of silver cations in aliphatic OH (TRIS) surface dendrimers followed by photolysis*
(Conjugation by complexation of transition metal ions followed by a zero-order monomolecular reaction.)

Preorganization mechanism:	Complexation in a homogenous ligand-field
Immobilization reaction:	(monomolecular, zero order) $Ag^+ + h\nu \Longrightarrow Ag(0)$
Dominant DNC interaction:	Dendrimer–Dendrimer (D↔D)
Result:	A low metal content and dominantly interior 'I' type nanocomposite

When transition metal cations are used that form complexes with the free electronpair of the unprotonated tertiary nitrogens located at the branching sites of PAMAM dendrimers, the distribution of metal ions is homogenous within the dendrimers because of the isotropic nature of the diffusion. Accordingly, the individual dendrimers will form complexes with an equal and well-defined number of metal atoms. The number is predetermined by the ratio of metal ion moles *per* dendrimer moles. When TRIS-modified PAMAMs are used, silver ions prefer the tertiary nitrogens to the aliphatic hydroxide and accumulate in the interior of the dendrimers. According to X-ray and neutron diffraction measurements [39–41], the size of the dendrimers usually is not altered by the complexation, but the electrostatic interactions between dendrimer–metal complexes are considerably decreased [42].

Silver–dendrimer nanocomposite was prepared by photolytic decomposition of silver acetate complexed in a PAMAM_E4.TRIS dendrimer. The solution of this complex proved to be quite insensitive to light: one day exposure to daylight of a glass vial containing 10 mM solution of $[(CH_3COOAg)_{31}$-PAMAM_E4.T] complex resulted in only approximately 50% conversion based on changes in the visible spectra. Extended exposure to light completed the photolysis and provided dark brown $\{Ag(0)_{31}$-PAMAM_E4.TRIS$\}$ solution.

Photolysis of these complexed silver ions generates metallic silver domains while maintaining the homogenous distribution. UV–visible spectrum (Figure 1) displays one major symmetric plasmon peak at 420 nm.

A representative TEM image of the {$Ag(0)_{31}$-PAMAM_E5.T} is shown in Figure 2. The large round objects on the selected image are polystyrene (PS) latex microspheres, which have been deposited with the dendrimers as scale markers. The two darker objects are a dendrimer–silver nanocomposite and a dendrimer–silver cluster. In this TEM image employing a mass–thickness contrast mechanism, the nanocomposites appear darker although their diameters are much smaller than the PS spheres and thus their thickness are much smaller than the PS spheres. This is clear evidence of metal incorporation into the dendrimers. The featureless image of the nanocomposites suggests an amorphous arrangement of the silver atoms within the dendrimers.

Interactions between the 'I'-type nanocomposite particles are dominated by the dendrimer–dendrimer surface interactions. It is characteristic to TRIS-terminated PAMAMs that the H-bonding between dendrimers leads to self-assembly in concentrations higher than 0.8% w/w [41]. What are the scaling factors for these higher order aggregates is not understood yet, but the same contrast (i.e., silver content) illustrates well the identical result of the identical forces within identical nanoparticles. Whether these aggregates are present in the original solution of the nanocomposites or the consequence of the TEM sample preparation process remains to be seen, and this phenomena is presently under investigation.

According to their featureless or very poor XRD spectra (not shown), these internalized metal/inorganic domains are amorphous or have a very low degree of crystallinity. Location of these domains depends also on the kinetics of the immobilizing reaction.

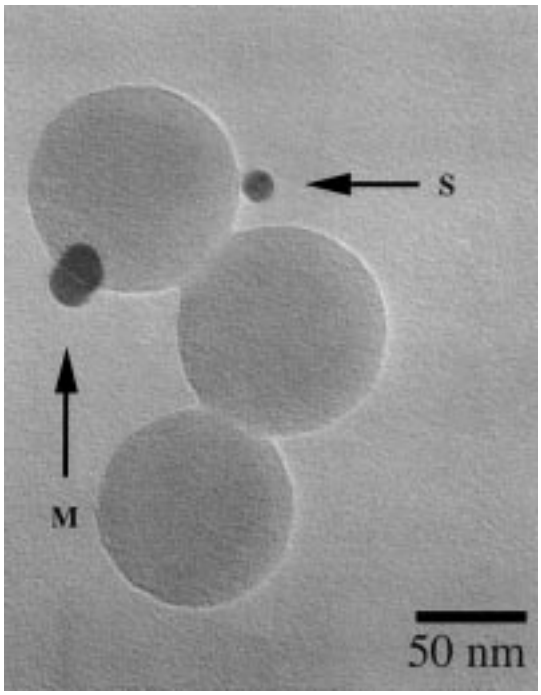

Figure 2. TEM image of {$Ag(0)_{31}$-PAMAM_E4.TRIS} nanocomposite particles. The three lighter objects, joined at the edges, are polystyrene spheres. The single nanocomposite (S) has a diameter of 14 nm and the multiple nanocomposite cluster (M) has a size of 28 by 20 nm.

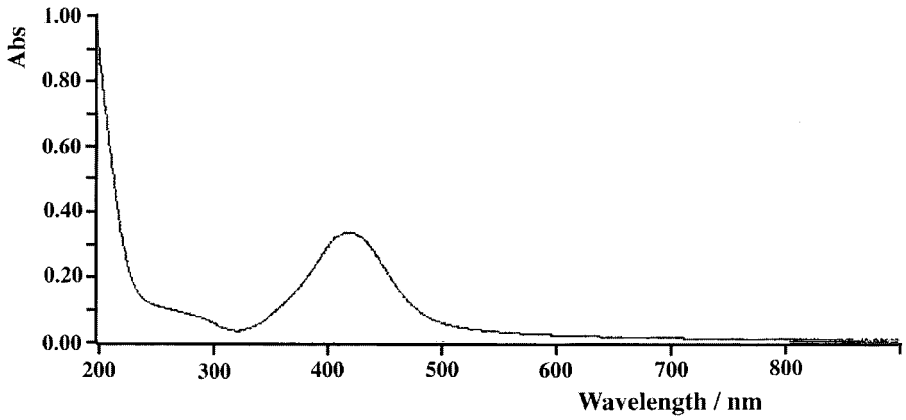

Figure 1. UV–visible spectra of {$Ag(0)_{31}$-PAMAM_E4.TRIS} nanocomposite solution in water.

We assume that when this reaction is a zero-order process, such as the photolysis of silver ions, metal atoms form at the same location where they were originally complexed. According to the TEM images, they did not migrate considerably within the time-scale of the investigation.

DNC-2 example: *Binding of silver cations by PAMAM carboxylates followed by chemical reduction* (Conjugation by salt formation between PAMAM dendrimer surface poly-anions and transition metal cations followed by a bimolecular chemical reaction.)

Preorganization mechanism:	Salt formation on a spheroidal carboxylate (anionic) exterior surrounding a homogenous (cationic) ligand-field
Immobilization reaction:	(bimolecular chemical reduction) $Ag^+ + e^- \Longrightarrow Ag(0)$
Dominant DNC interaction:	Guest–Guest (G↔G)
Result:	A high metal content 'E' (exterior) type nanocomposite containing different size multiplets of equally loaded single dendrimer units.

Due to their architecture, medium and high generation PAMAM dendrimers are generally unable to interpenetrate, and behave as separate spheres [43]. Carboxylate-terminated dendrimers are interesting examples of a Janus-faced macromolecule, in which the interior contains a high local concentration of tertiary nitrogens with lone electronpairs (proton-acceptors), while the surface is covered with weakly dissociated carboxylate groups (proton-donors). Carboxylated Starburst® dendrimers strongly interact with positively charged molecules [44,45] or surfaces, but they are also known to behave as non-interacting spheres during chromatography in the presence of an appropriate aqueous mobile phase [46]. This non-interacting behavior is due to the negatively charged dendrimer surfaces which repel each other, regardless of whether the salt or acid forms are dominant.

When insoluble silver acetate was added to the aqueous solution of the TRIS modified dendrimer, it quickly dissolved, but when silver nitrate solution was added to the carboxylate terminated PAMAM, a white salt precipitated. This precipitate dissolved only after several days. We speculate, that carboxylates are weak acids and therefore most of the silver ions are present at first in undissociated forms, i.e., on the surface of the template. However, nitrogens under the carboxylate layer remained able to form multidentate cationic complexes with silver, which later resulted in soluble nanocomposites. Of course, in both cases the equilibrium character is preserved resulting a mixed ('M') type nanocomposite in which both the interior and the exterior contributes to hosting the silver ions, although according to a different mechanism. This mixed template mechanism results in higher metal ion binding capacity (a generation five PAMAM carboxylate dendrimer was able to contain up to 150 silver atoms per dendrimer molecule) but generates more complex nanocomposite structures upon immobilization. We believe that size distribution differences due to the formation mechanism are also reflected in these more irregular images.

Comparison of the UV–visible spectra also suggests this difference. In an otherwise identical local environment, the position of the observed dispersion peak for nanoparticles is the function of the domain size and the aspect ratio [3]. Consequently, one expects a single distribution curve in the electromagnetic spectra for a homogenous particle and the resultant of several different curves (therefore broader and much less defined) for a nanoparticle system that has multimodal distribution [13]. $\{Ag(0)_{31}$-PAMAM_E4.TRIS$\}$ forms an 'I' type nanocomposite, because (a) silver ions prefer the nitrogen ligands to the surface OH groups, and (b) the immobilization was caused by a photochemical reduction which is not site-specific. However, $\{Ag(0)_{150}$-PAMAM_E5.COOH$\}$ constitutes an 'E'-type nanocomposite, because Ag^+ is more preferred by the surface carboxylate groups than the internal nitrogens. In addition, the immobilization reaction in this case was a reduction with a slight excess of hydrazine. Since this reactant encounters the preorganized ions from *outside* of the dendrimer molecules, the primary location of reaction will be the periphery and the exterior of the host molecule, similarly to the case of copper sulfide nanocomposites [40].

Comparison of UV–visible spectra of these silver nanocomposite solutions illustrates well the expected difference between the single peak spectrum of the internalized silver nanodomains in the 'I' case and the

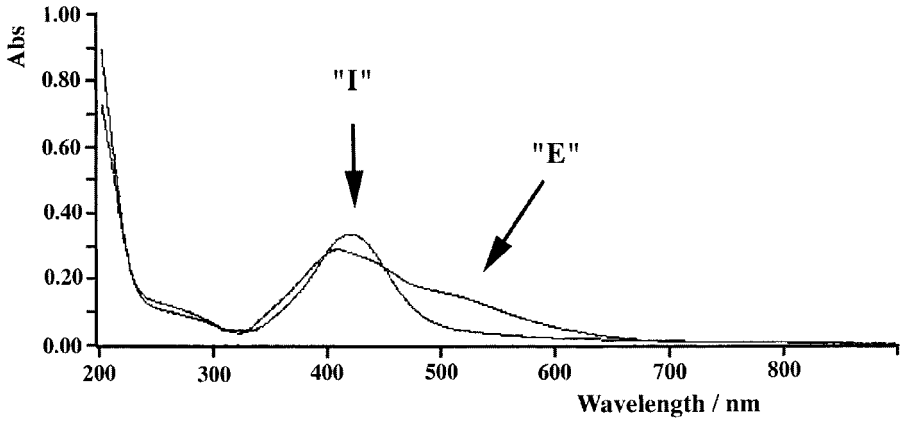

Figure 3. Comparison of the UV–visible spectra of {$Ag(0)_{150}$-PAMAM_E5.COOH} ('E'-type) and {$Ag(0)_{31}$-PAMAM_E4.T} ('I'-type) nanocomposite solutions in methanol.

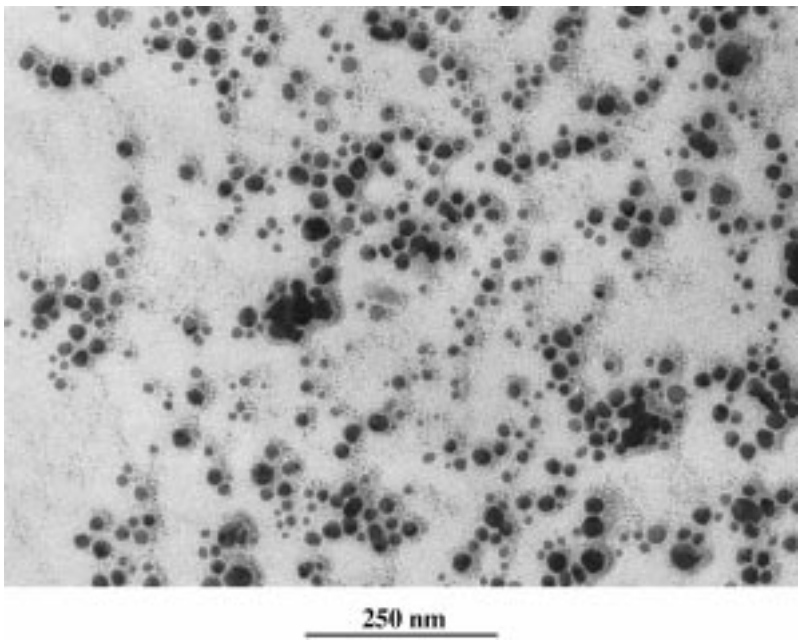

Figure 4. Overview of the {$Ag(0)_{150}$-PAMAM_E5.COOH} TEM image.

presence of a more heterogeneous size-distribution in the external one (Figure 3).

The formation mechanism of {$Ag(0)_{150}$-PAMAM_E5.COOH} often gives rise to multiple nanocomposite units (containing several dendrimers surrounded with and connected by silver nanoshells) resulting in more complex spectral peaks (see also TEM image on Figure 4).

HRTEM image of the individual {$Ag(0)_{150}$-PAMAM_E5.COOH} nanocomposites (Figure 5, A) in some cases suggested the 'collapse' of the silver domains toward the interior of the nanoparticles. In addition, inhomogenous scattering *between* the associated host molecules may be noticed (Figure 5, B). In Figure 5, the three individual dendrimer nanocomposites on the right-hand-side of the image have the same

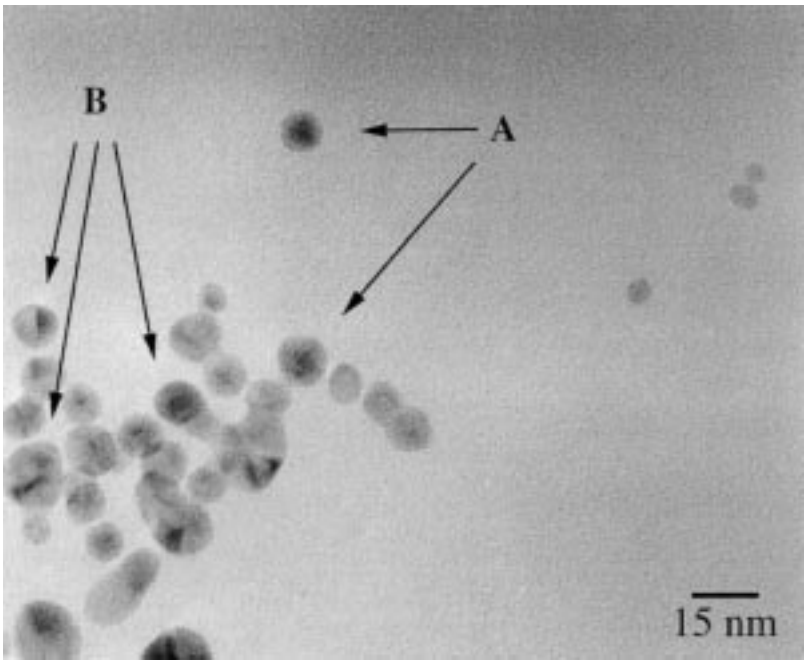

Figure 5. Hr TEM image of a $\{Ag(0)_{150}$-PAMAM_E5.COOH$\}$ nanocomposite. See explanation for A and B in the text.

kind of structure as in Figure 2, where the metal is incorporated into the dendrimers and is not crystalline. The larger clusters on the left-hand-side of the image contain dark spots and bands present in the image. These dark patterns are indicative of diffraction contrast caused by a metal crystalline lattice. It thus appears that the surface-positioned silver has formed very small nanocrystalline regions by means of adhering single nanocomposite units together.

TEM images acquired from more concentrated nanocomposite solutions show large (>1 micron) silver clusters (not shown). However, even after thorough drying, the resulting black solid nanocomposite remained soluble in water. As zerovalence silver would crystallize into insoluble clusters, these nanocomposite particles must be separated by organic domains and must have at least part of their dendrimer surface accessible for the solvent. This observation also supports a possible slow movement of silver atoms into the interior of the nanocomposite particles.

DNC-3 example: *Salt formation between tetrachloroaurate anions and cationic PAMAM dendrimers followed by disproportionation or reduction into dendrimer–gold nanocomposites*
(Salt formation between complex anions and cationic sites of PAMAM dendrimers followed by a monomolecular or bimolecular reaction.)

Preorganization mechanism:	Salt formation on a spheroidal carboxylate (cationic) exterior surrounding a homogenous (cationic) ligand-field.
Immobilization reaction:	Monomolecular decomposition or bimolecular chemical reduction.
$[AuCl_4]^- \Longrightarrow AuCl_3 + HCl \Longrightarrow [AuCl_3OH]^-$, etc.	
Dominant DNC interaction:	Guest–Guest (G↔G)
Result:	Interior ('I'), mixed ('M') or exterior ('E') type $\{Au(0)\}$ nanocomposites depending on the actual metal content and the procedure used.

Noble metals, especially gold, have many applications in optical and biological sciences due to its stability. Gold is extensively used on electrode surfaces and as a base-layer for self-assembled monolayers [47]. Metallic gold are usually produced by reduction using

Na-citrate, citric acid, hydrazine, hydrogen or electrochemical deposition, and the color is the function of size and shape of the metal domains formed [13]. Spectral characteristics and nonlinear optical properties of gold nanolayers/rods/particles are well investigated from both theoretical and experimental point of view.

Use of PAMAM dendrimers as platforms for the deposition of gold colloid monolayers on various substrates allowed an unusual degree of control and uniformity [48].

Preorganization of the gold atoms with dendrimers has been carried out by mixing aqueous dendrimer and $[AuCl_4]^-$ solutions in calculated ratios [49]. The yellow $[AuCl_4]^-$ solution lost its yellow color immediately upon mixing with the PAMAM indicating a change in the electronic environment of the tetrachloroaurate counterion, i.e., the formation of a salt between the dendrimer nitrogens and a multiple complex anion, $[(PAMAM\_E5.NH_2)\ [AuCl_4]_{10}{}^-]$. (Formation of other hydrolysis products, such as $AuCl_3OH,^-$ or different cationic four-coordinate tetrachloroaurate depending on concentration and pH are also possible on the analogy of the reaction with diethylenetriamine may also be possible) [50]. In the ammonium salt formation between dendrimers and complex anions of transition metals a polycationic amino surface dendrimer acts as preorganizer for the anions and salt-formation occurs with the dendrimers. Structure of the resulting polysalt is the function of the dendrimer architecture, i.e., whether the dendrimer surface is able or unable to interact with the precursor anion. The reaction may be continued by allowing a slow disproportionation reaction of the $Au_2O_3 \times H_2O$ or with reducing the immobilized gold ions into metallic gold with any conventional reducing agent. If not reduced, in the basic environment of the PAMAM interior the complex anion slowly loses HCl from the complex anion to the dendrimer nitrogens and gradually becomes immobilized by the subsequent hydrolysis. Due to this complex reaction mechanism, the temperature, reagent ratios, concentrations and the order of addition are also influences of the product structure. Solubility and stability of the obtained $\{Au(0)_{10}$-PAMAM, E5.0$\}$ gold nanocomposites were determined by the solubility of the host dendrimer molecule. UV–visible spectra of this nanocomposite showed a plasmon peak [36,49,51] at 532 nm (Figure 6).

According to literature data on 'hard' nanoparticles [52], appearance of a plasma absorption band in classical gold colloids is an indication of a particle size larger than 2 nm. Diameter of the PAMAM E5.0 equals to 54 Å [53], thus these optical measurements confirm that the sizes of the metallic domains of dendrimer nanocomposites are in the nanometer ranges. What is the location of the gold atoms in this nanocomposite? Apparently, ten to fifteen metal atoms cannot cover the surface of a dendrimer with a 54 Å diameter.

High resolution TEM micrograph of a $\{Au(0)_{10}$-PAMAM, E5.0$\}$ gold nanocomposite clearly demonstrates that the sizes of the gold metal domains were templated by the PAMAM dendrimers. When limited number of gold atoms are present in a PAMAM dendrimer, the metallic domains appear as an inverse image of the shape, and size-distribution of the host dendrimer (Figure 7).

It also has to be mentioned, that average diameter of PAMAM dendrimers is different from the diameters determined by scattering methods [53] in solution.

This HRTEM image also shows spherical particles with all the three possible structures present. Within the single gold nanocomposite particles (depending

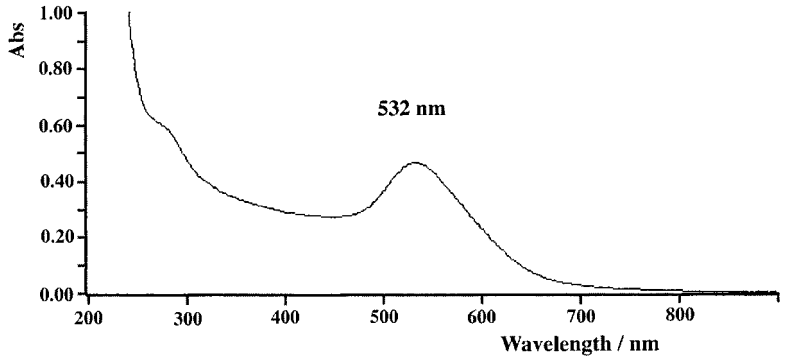

Figure 6. UV–visible spectrum of a $\{Au(0)_{10}$-PAMAM_E5.$NH_2\}$ nanocomposite after seven days (gold concentration is 0.5 mg/ml).

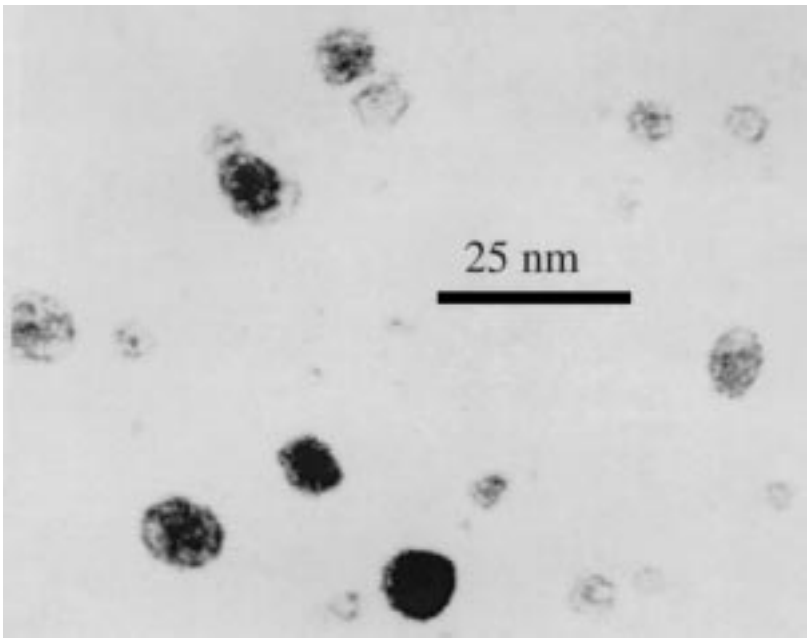

Figure 7. Hr TEM image of a $\{Au(0)_{10}$-PAMAM_E5.$NH_2\}$ gold–dendrimer nanocomposite.

on the degree of metal loading) gold may be found either *inside* of the dendrimer molecule, or *on* the dendrimer molecule, or both on the surface and inside, similarly to the DNC-2 silver case. The individual metal–dendrimer ratios are determined by the local reagent ratios during mixing.

The obtained structural pattern depends also on the reactant ratio. Figure 8 shows a surface-plot of a $\{Au(0)_{24}$-PAMAM, E5.0$\}$ gold nanocomposite TEM image analyzed by the 'NIH Image' software. The base diameters on this plot are proportional to the particle size, and the height is proportional to the optical density, i.e., the metal concentration.

Despite of the nearly uniform distribution of the single gold nanocomposite units, it is obvious that there are two different distributions present in the sample. One of the distributions is the consequence of the instant decomposition (i.e., immobilization) of the gold compounds during mixing (distribution in particle loading) and the second is caused by the metal–metal interactions on the dendrimer surface resulting from the bimolecular nature of the reduction (distribution in particle diameter).

Finally, formation of secondary structures and higher order assemblies between single dendrimer nanocomposite particles has also been detected, similar to classical clusters of 'hard' nanocrystalline particles. (In this paper we use the term 'cluster' to identify multiples of elemental nanocomposite particles held together by physical forces.) This clustering process of nanocomposites largely depends on their composition, architecture, surface and local environment. For example, it was observed [32,39], that $\{(CuS)_{31}$-PAMAM_E4.TRIS$\}$ and $\{(Cu_2S)_{15}$-PAMAM_E4.TRIS$\}$ aliphatic hydroxyl surface dendrimer based copper sulfide nanocomposite singlets self-organized into about 100 nm diameter composite clusters containing $\{CuS\}$ or $\{Cu_2S\}$ nanocomposite particles connected by their peripheral copper sulfide content upon storing their aqueous solutions at room temperature for three days [40].

This cluster formation occurs through the interaction of the nanocomposite surfaces. In the case of external type metal nanocomposites, these physical clusters are composed of well-defined size nanoshells touching each other. In Figure 9 several examples of single, double, triple and higher degree of clustering of 'E'-type gold nanoshells are shown, in addition to an example of dimerized superclusters containing approximately 50–60 single units.

It is also possible to organize single nanocomposite units into higher hierarchies through chemical surface interactions. To a gold nanocomposite solution of $\{Au(0)_{10}$-PAMAM_E5.$NH_2\}$ (see TEM in Figure 10A) a dilute bromine solution was added in

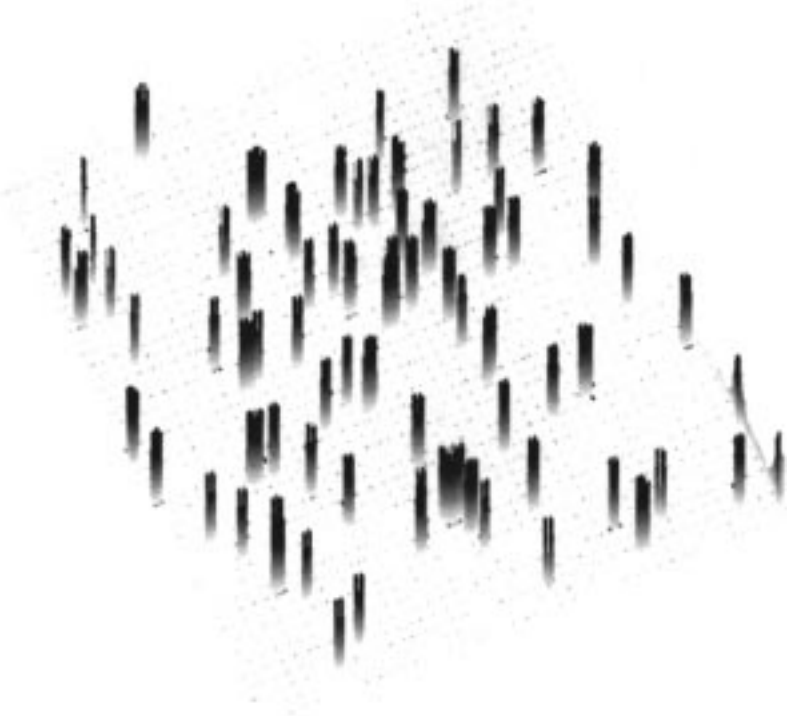

Figure 8. Surface plot representation of a TEM image acquired from a {$(Au(0)_{24}$-PAMAM_E5.NH_2} nanocomposite sample.

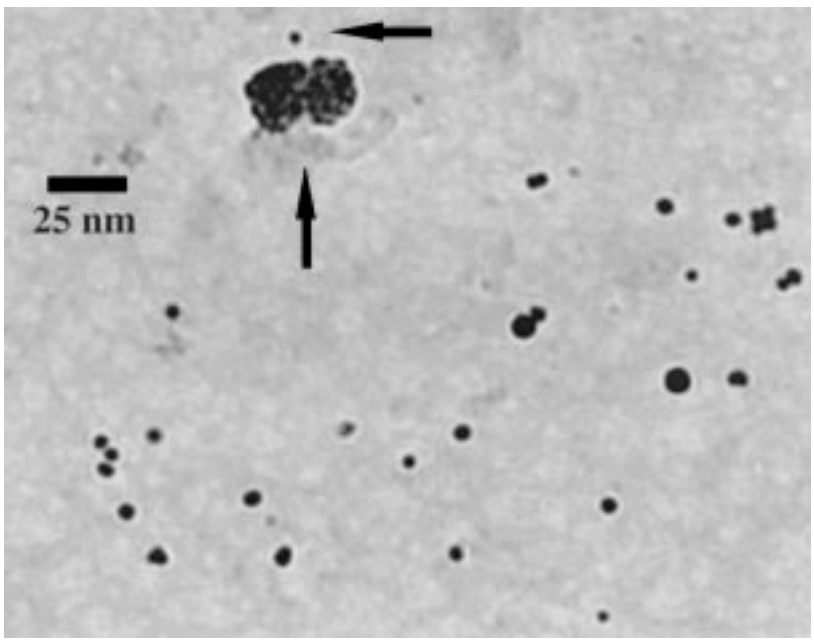

Figure 9. Different surface clustering of a {$(Au(0)_{24}$-PAMAM_E5.NH_2} nanocomposite unit as shown by its TEM.

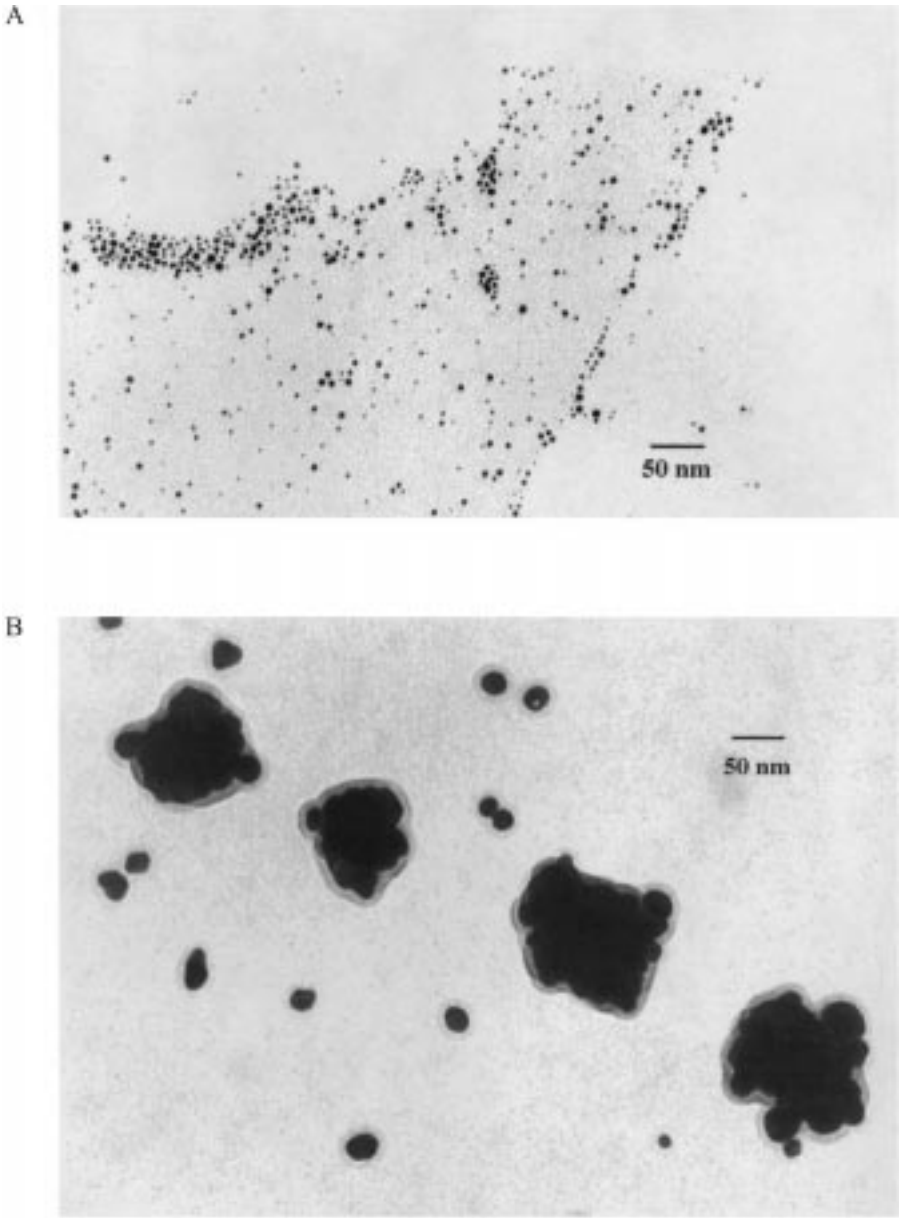

Figure 10. TEM image of a $\{Au(0)_{24}$-PAMAM_E5.$NH_2\}$ nanocomposite before (A) and after (B) reacting the nanocomposite with slight excess of bromine in aqueous solution.

methanol (equimolar to the concentration of primary amino groups), which, instead of a continuous distribution, led to the formation of larger particles depicted in Figure 10B. Formation of only two major sizes (clusters and 'superclusters' thereof) were observed from the primary clusters. This phenomenon apparently demonstrates the importance of scaling rules in the process of physical clustering in dendrimer nanocomposites, similarly to the 'magic numbers' [38].

Very little is known about the physics and chemistry of clusters and nanocomposites based on dendritic polymers yet. Observations, rules and theory that are valid for conventional metal clusters (which are composed of *microcrystalline* metals) are for comparison

only because of the different structure of these 'soft' clusters. Further investigation of this and similar processes is part of our ongoing research to understand better the properties and manipulation of these extremely useful materials.

Conclusions

In this paper, typical formation mechanisms of DNCs have been investigated. Depending on the composition and architecture of the dendrimer template and on the mechanism and kinetics of the preorganization and immobilizing reactions, different nanocomposite structures may form. The inorganic component may primarily be scattered either in the dendrimer interior, or may be dispersed under the surface as well as on a surface 'shell' or both. The formed nanomaterials have been described as internal ('I'), external ('E') and mixed ('M') nanocomposites. The resulting primary structures may assemble to give structures of higher hierarchies.

The versatility of the dendrimer technology combined with the vast experience of inorganic chemistry provides unlimited possibilities in the synthesis of novel nanomaterials and unprecedented control over these systems. We expect, that it will be possible to build well-defined and precise nanoscale inorganic objects by utilizing perfect organic templates. The endless variations of possible dendritic architectures and easy availability of dendrimer based nanocomposites may generate a new and very practical knowledge in several scientific areas including chemistry, materials science and physics, as well as in the interdisciplinary fields of cluster science and nanotechnology.

Acknowledgements

This work was performed at the ARL-MMI Dendrimer Center of Excellence sponsored by the Army Research Laboratory under the contract of DAAL-01-1996-02-0044. High resolution TEM measurements were carried out at the W.M. Keck Electron Microscopy Laboratory at the University of Massachusetts Amherst. Support for this work was obtained from the MRSEC central facilities at the University of Massachusetts and from the Army Research Office under contract DAAE55-98-1-0116.

Thanks are expressed to colleagues at MMI: Dr. Douglas R. Swanson for kindly providing the functionalized PAMAM dendrimers and to Mr. Kevin Battjes for X-ray diffraction and TEM measurements. Authors also thank Drs. Nora Beck Tan (ARL) and Sam F. Trevino (ARL) for their interest and valuable comments.

References

1. R&D Status and Trends in Nanoparticles, Nanostructured Materials and Nanodevices in the United States, Proceedings of the May 8–9, 1997 Workshop. International Technology Research Institute, 1998.
2. Drexler, K.E., Nanosystems, Wiley-Interscience, NY–Chicester–Brisbane–Toronto–Singapore, 1992.
3. Alivisatos, A.P., Science, 271, 923, 1996.
4. *Physics and Chemistry of Metal Cluster Compounds* L.J. de Jongh (ed.) Kluwer Academic, Dordrecht/Boston/London, 1994, and references thereof.
5. Schmid, G., Chem. Rev., 92, 1709, 1992.
6. Schmid, G. and Hornyak, G.L., Current Opinion in Solid State and Mat. Sci., 2(2), 204, 1997.
7. Cohen, M.L. and Knight, W.D., Physics Today, 12, 42, 1990.
8. Frens, G., Nature Phys. Sci., 241, 20, 1973.
9. Fendler, J.H. and Meldrum, F.C., Adv. Mater., 7(7), 607, 1995.
10. Petit, C., Lixon, P. and Pileni, M.P., J. Phys. Chem., 97, 12974, 1993.
11. Calvert P. and Rieke P., Chem. Mater., 8, 1715, 1996.
12. Douglas, T., Dickson, D.P.E., Betteridge, S., Carnock, J., Garner C.D. and Mann, S., Science, 269, 54, 1995.
13. Martin, C.R., Science, 1994, 266 (December 23), 1961.
14. Markowitz, M.A., Chow, G.-M. and Singh, A., Langmuir, 199, 10, 4095.
15. Amundsen, A.R., Whelan, J. and Bosnich, B., J. Am. Chem. Soc., 99(20), 6730, 1977.
16. Mirkin, C.A., Letsinger, R.L., Mucic, R.C. and Storhoff, J.J., Nature, 382, 607, 1996.
17. Andrews, M.P. and Ozin, G.A., Chem. Mater., 1, 174, 1989.
18. Huang, H.H., Yan, F. Q., Kek, Y.M., Chew, C.H., Xu, G.Q., Ji, W., Oh, P.S. and Tang, S.H., Langmuir, 13, 172, 1997.
19. Kuczynski, J.P., Milosavljevic, B.H. and Thomas, J.K., J. Phys. Chem., 88, 980, 1984.
20. Moffitt, M., McMahon, L., Pessel, V. and Eisenberg, A., Chem. Mater., 7, 1185, 1995.
21. Fogg, D.E., Radzilowski, L.H, Blanski, R., Schrock, R.R. and Thomas, E.L., Macromolecules, 30, 417, 1996.
22. Spatz, J.P., Sheiko, S. and Moller, M., Macromolecules, 29, 3220, 1996.
23. Gorman, C.B., Parkhurst, B.L., Su, W.Y. and Chen, K., J. Am. Chem. Soc. 119(5), 1141, 1997.
24. Chu, A., Cook, J., Heesom, R.J.R., Huchison, J.L., Green, M.L.H. and Sloan, J., Chem. Mater., 8, 2751, 1996.
25. Gray, D.H., Hu, S., Juang, E. and Gin, D.L., Adv. Mater., 9(9), 728, 1997.

26. Pileni, M.P., Langmuir, 13, 3266, 1997, and, ibid., 3927.
27. (a) Tomalia, D.A., Baker, H., Dewald, J., Hall, M., Kallos, M., Martin, S., Roeck, J., Ryder, J. and Smith, P., Polym. J. (Tokyo) 17, 117–132, 1985, (b) Tomalia, D.A., Naylor, A.M. and Goddard III, W.A., Angew. Chem., 102(2), 119–157, 1990, Angew. Chem. Int. Ed. Engl. 29(2), 138–175, 1990.
28. Dandliker, P.J., Diederich, F., Gross, M., Knobler, C.B., Louati, A. and Sanford, E.M., Angew. Chem. Int. Ed. Engl. 33, 17, 1739, 1994.
29. Valerio, C., Fillaut, J., Ruiz, J., Guittard, J., Blais, J. and Astruc, D., J. Am. Chem. Soc. 119(10), 2588, 1997.
30. Slany, M., Bardaji, M., Caminade, A., Chaudret, B. and Majoral, J., Inorg. Chem. 369, 1939, 1997.
31. Tomalia D.A. and Balogh, L., U.S. Patent Application 08/924,790 September 5, 1996.
32. Balogh, L., Swanson, D.R., Spindler, R. and Tomalia, D.A., Proc. ACS PMSE, 77, 118, 1997.
33. Balogh, L. and Tomalia, D.A., J. Am. Chem. Soc., 120(29), 7355, 1998.
34. Zhao, M., Sun, L. and Crooks, R.M., J. Am. Chem. Soc., 120(19), 4877–4878, 1998.
35. Sooklal, K., Hanus, L.H., Ploehn, H.J. and Murphy, C.J., Adv. Mater., 10(14), 1083, 1998.
36. Esumi K., Suzuki, A., Aihara N., Usui, K. and Torigoe K., Langmuir, 14, 3157–3159, 1998.
37. Balogh, L. and Tomalia, D.A., Adv. Mater., 1999, submitted for publication.
38. *Physics and Chemistry of Metal Cluster Compounds* L.J. de Jongh, (ed.) Kluwer Academic, Dordrecht/Boston/London, 1994, and references thereof.
39. Beck Tan, N., Balogh, L. and Trevino, S., Polym. Mater. Sci. & Eng., 77, 120, 1997.
40. Beck Tan, N., Balogh, L., Trevino, S., Tomalia, D.A. and Lin, J.S., Characterization of Dendrimer-based Nanocomposites by SAXS and SANS. In Hybrid Materials, Mat. Res. Soc. Symp. Proc., 519, 143–150, 1998.
41. Beck Tan, N., Balogh, L., Trevino, S., Tomalia, D.A. and Lin, J.S., Polymer, 40, 2537–2545, 1999.
42. Balogh, L., Swanson, D.R., Fry, J. and Tomalia, D.A., 1998, submitted to Industrial and Engineering Chemistry Research.
43. Uppuluri, S., Ph.D. Thesis, Michigan Technological University, 1998.
44. Li, Y., Dubin, P.L., Spindler, R. and Tomalia, D.A., Macromolecules, 28, 8426, 1995.
45. Zhang, H., Dubin, P.L., Spindler, R. and Tomalia, D.A., Ber. Bunsenges. Phy. Chem. 100(6), 923, 1996.
46. Dubin, P.L., Edwards, S.L., Kaplan, J.I., Mehta, M.S., Tomalia, D.A. and Xia, J., Anal. Chem. 64, 2344, 1992.
47. Colvin, V.L., Goldstein, A.N. and Alivisatios, A.P., J. Am. Chem. Soc., 114, 5221, 1992.
48. Bar, G., Rubin, S., Cutts, R.W., Taylor T. N. and Zawodinski, T.A. Jr., Langmuir, 12, 1172, 1996.
49. He, Jin-An, Yang K., Valluzzi, R., Samuelson, L., Kumar, J., Tripathy, S.K., Balogh, L. and Tomalia, D.A., Chemistry of Materials, 1999, in press.
50. Cotton and Wilkinson: *Advanced Inorganic Chemistry*, Fourth Ed., J. Wiley and Sons, 1980.
51. Mie, G., Ann. Phys., 25, 377, 1908.
52. Doremus, R.H. and Rao, P., J. Mater. Res., 11(11), 2834, 1996.
53. (a) Bauer, B.J., Briber, R.M., Hammouda, B. and Tomalia, D.A., PMSE 67, 428, 1992, (b) Prosa, T.J., Bauer, B.J., Amis, E.J., Tomalia, D.A. and Scherrenberg, R., J. Polym. Sci., Polym. Phys. Ed. Part B, 35, 2913, 1997.